

Cross-Level Sensor Fusion with Object Lists via Transformer for 3D Object Detection

1st Xiangzhong Liu
fortiss GmbH
 Munich, Germany
 xliu@fortiss.org

2nd Jiajie Zhang
Technical University of Munich
 Munich, Germany
 jiajie.zhang@tum.de

3rd Hao Shen
fortiss GmbH
 Munich, Germany
 shen@fortiss.org

arXiv:2512.12884v2 [cs.CV] 25 Jan 2026

Abstract—In automotive sensor fusion systems, smart sensors and Vehicle-to-Everything (V2X) modules are commonly utilized. Sensor data from these systems are typically available only as processed object lists rather than raw sensor data from traditional sensors. Instead of processing other raw data separately and then fusing them at the object level, we propose an end-to-end cross-level fusion concept with Transformer, which integrates highly abstract object list information with raw camera images for 3D object detection. Object lists are fed into a Transformer as denoising queries and propagated together with learnable queries through the latter feature aggregation process. Additionally, a deformable Gaussian mask, derived from the positional and size dimensional priors from the object lists, is explicitly integrated into the Transformer decoder. This directs attention toward the target area of interest and accelerates model training convergence. Furthermore, as there is no public dataset containing object lists as a standalone modality, we propose an approach to generate pseudo object lists from ground-truth bounding boxes by simulating state noise and false positives and negatives. As the first work to conduct cross-level fusion, our approach shows substantial performance improvements over the vision-based baseline on the nuScenes dataset. It demonstrates its generalization capability over diverse noise levels of simulated object lists and real detectors.

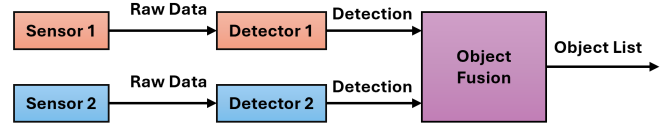
Index Terms—Sensor Fusion, Transformer, Object List, Automated Driving, V2X

I. INTRODUCTION

3D object detection is fundamental in autonomous driving and robotics. While vision-based methods have advanced, sensor fusion remains crucial for robust perception in dynamic scenarios by combining the strengths of multiple sensor modalities. Multi-sensor fusion systems are commonly categorized into three primary architectures based on different levels of abstraction: low-level, intermediate-level, and high-level fusion [1], respectively fusing raw sensor signals, extracted features, and decisions or object lists. Low-level fusion theoretically offers optimal state estimation [2]–[4], where recent advancements in deep neural networks (DNNs), particularly Transformers, have shown transformative capability.

V2X technology is widely involved in collective perception for autonomous driving [5], where the demand for data transmission efficiency has constrained the usability of low-level fusion. Furthermore, smart sensors [6] process data internally, such as MobileEye vision systems and Continental radars, and output only perceived object states other than raw data [7]. In these situations, fusion is only conducted at a high level [8].

Object-level (High-level) Fusion:



Data-level (Low-level) Fusion:



Cross-level Fusion:

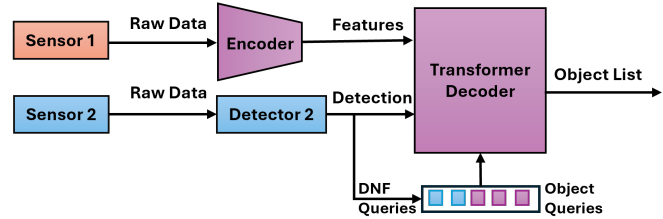


Fig. 1: A brief illustration of 3 multi-sensor fusion strategies. In object-level fusion, distributed object detectors send the source object lists to a central fuser to generate a final set of detected objects. Conversely, in data-level fusion, data from multiple sensors are fed into a central fusion system to perform object detection. Cross-level fusion combines these approaches, comprehensively utilizing information from representations at different levels to enhance detection performance.

No previous research has explored using end-to-end learning-based methods to fuse object lists with raw sensor data.

Cross-level fusion refers to integrating high-level information to low-level feature fusion as illustrated in Fig. 1. To achieve this, we extend DETR-like 3D object detection frameworks by embedding object lists as DN queries. Moreover, we explicitly convert object lists’ positional and dimensional information into an attention-weighting mask in the Transformer decoder. Treating the fusion process as an integral model rather than a separate step, as in high-level fusion, the framework can potentially create synergistic effects and achieve better efficiency and improved overall performance. High-level infor-

mation offers context for interpreting raw sensor data, while raw data provides fine-grained feature details missing from the abstracted representations, reducing state estimation errors.

We define object lists as structured sets of object detections containing position (x, y, z) , size (l, w, h) , orientation (yaw) , velocity (v_x, v_y) , and class information with estimation errors. The cross-level fusion facilitates object detection by leveraging prior information from object lists. Consequently, we validate its performance using the nuScenes dataset [9]. Our approach significantly outperforms the vision-based baseline, revealing the substantial advantages of early integration of highly abstract information with raw sensor data.

In summary, the main contributions of this paper include:

- 1) We are the first to introduce the concept of cross-level sensor fusion with a Transformer-based framework for 3D object detection, combining data modalities of different abstraction levels in an end-to-end manner other than only at the high level.
- 2) We leverage query denoising and explicit attention directing to implicitly and explicitly fuse object lists with raw image data. The approach integrates seamlessly into DETR-like 3D detectors as a plug-and-play module, requiring no additional parameters or computation, assuming a query-based architecture that supports attention-based conditioning.
- 3) As no public dataset contains object lists as a standalone modality, we developed a pseudo object list generation (POLG) module that introduces diverse state noise, false positives and negatives to ground truth, simulating object detectors with varying performance levels.

II. RELATED WORK

A. Object-level Fusion and Data-level Fusion

In object-level fusion (OF) distributed object detectors send the source object lists (object state estimation with error covariance) to a central fuser for more accurate decisions [1], as shown in Fig. 1. OF often deploys explicit data association and Bayesian methods, like the Kalman filter with diverse motion models.

OF enhances redundancy by incorporating multiple sensor sources, ensuring system reliability when facing individual sensor failure. Besides, it improves computational efficiency by reducing the data volume processed, as the fusion operates on structured object detections rather than raw data. Furthermore, object fusion facilitates modular scalability, allowing for the seamless integration of additional sensors into the system without significant architectural modifications [7], [10]. However, OF often faces data association errors due to limited object information, causing object state estimation inaccuracies.

In contrast, data-level fusion fully leverages detailed low-level data [10]. Typically implemented using deep learning models, it follows three main approaches: early fusion, where raw sensor data is unified; late fusion, where data is processed separately before merging decisions; and intermediate fusion,

which integrates features at an intermediate stage, balancing data interaction with computational efficiency [11]. However, these methods are designed for dense and reach positional data like point clouds and are not directly applicable to object lists, which contain sparse, explicit information, such as bounding boxes. To effectively fuse object lists, alternative strategies are needed to harness their structured, concise nature.

B. Two-stage Detection and Proposal-level Fusion

The two-stage detection process typically involves two main steps: region proposal and region classification [12]. Initially, the system processes sensor data to produce feature maps, which are used to identify regions of interest (RoIs) by projecting 3D bounding boxes onto 2D feature maps. These methods use the object hypotheses generated in the initial detection stage to refine and validate object positions, enhancing the overall accuracy and robustness of the detection system. Notable works like MV3D [13] and AVOD [14] deploy multi-view aggregation for detection, while other methods incorporate Transformer decoders for advanced fusion. FUTR3D [15] emphasizes a unified query structure called Modality-Agnostic Feature Sampler across different modalities and incorporates a Transformer decoder to avoid late fusion heuristics. TransFusion [16] fuses LiDAR and image data, with the first decoder layer predicting bounding boxes from LiDAR and the second adaptively integrating image features. An image-guided query initialization strategy further enhances the detection of objects that are challenging to identify in point clouds. FusionRCNN [17] utilizes RoIPooling to obtain data samples within proposals and then employs intra-modality self-attention to enhance domain-specific features and a cross-attention mechanism to align both modalities. However, the region proposals and object queries, usually of a significant amount than the ground truth, still originate from raw data or features, which inherently contain substantially richer information and redundancy compared to the object lists.

III. METHODOLOGY

The main aim is to implement a cross-level sensor fusion approach to fuse object list information with camera data end-to-end. For the overall architecture as shown in Fig. 2, we retained the main structure of our baseline PETRv2 [18], due to its query-based design and temporal modeling through a 3D position-aware attention mechanism. Images $I = \{I_i \in \mathbb{R}^{3 \times H_I \times W_I}, i = 1, 2, \dots, N\}$ from N camera views are processed by a backbone network (e.g., VoVNetCP [19]) to extract 2D multi-view features $F^{2d} = \{F_i^{2d} \in \mathbb{R}^{C \times H_F \times W_F}, i = 1, 2, \dots, N\}$. 3D coordinate generator discretizes the camera frustum space into a 3D meshgrid, transforming these coordinates into the 3D world space using camera parameters. 2D features and 3D coordinates from neighboring frames are concatenated and processed by the 3D position encoder (PE) to generate 3D position-aware features. These features serve as keys and values in the Transformer decoder.

We exploit object-centric query denoising (QDN) with object lists by combining denoising and learnable queries,

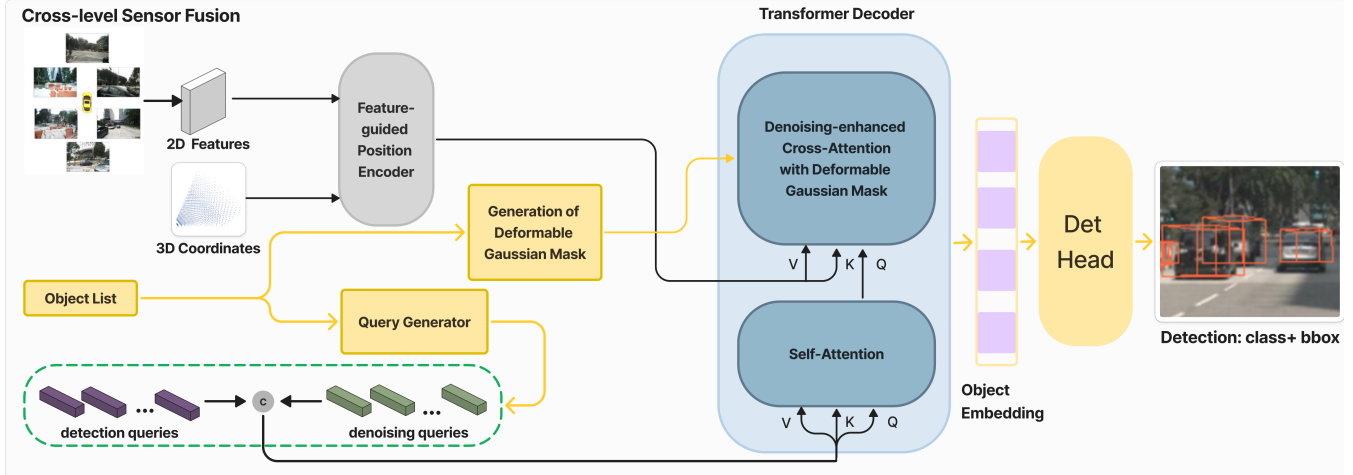


Fig. 2: The illustration architecture of our overall cross-level fusion framework for 3D object detection. In particular, DN queries from object lists are concatenated with detection queries from camera data to form denoising queries, which are fed into the self-attention module of the Transformer decoder for modality alignment. The information represented in the object lists is introduced into Transformer’s cross-attention module using deformable multi-view multi-target Gaussian masks, which correlate with the 3D object representations from camera data through denoising processes. This approach facilitates more precise object positioning and classification. The object embeddings from the Transformer outputs are then processed by the detection head to generate object bounding boxes.

which interact further with feature and positional encoding to extract object embeddings for detection. QDN reduces state uncertainty in the original object list and enriches DN queries by incorporating image features. Explicit attention directing utilizes positional and spatial information of the object list to create soft connections between the object priors and multi-view image features during cross-attention.

To simulate realistic black-box detectors, we generate pseudo object lists with stochastic variations by sampling the ground truth bounding boxes (position, size, orientation, velocity, and labels). We apply configurable noise, including Gaussian position/size noise, object drops (detection failures), false positives (spurious detection), and label misclassification. Noise levels vary randomly within set limits to better mimic estimation errors and detection inaccuracies. However, real-world object lists could introduce additional uncertainty, which may affect fusion performance. Addressing this requires to selectively trust object lists based on confidence scores or consistency across frames.

A. Object-centric Query Denoising

Object-centric query denoising is firstly introduced in DN-DETR [20] to tackle the issues with the instability of bipartite graph matching and inconsistent optimization goals during early training stages of DETR. This method initializes queries with noisy ground-truth bounding boxes, termed “denoising queries”, aiming to reconstruct the original, clean boxes. The mechanism of DN-DETR series aligns with our assumption for cross-level fusion of object lists with raw sensor data using Transformers. The object list can be seen as noisy samplings of the ground truth with with estimation errors, FPs, and FNs, which can be directly converted to DN queries

for DETR-like detectors. Besides, the built-in data processing systems to produce the object lists are black box, providing no information to de-correlate the object lists for optimal fusion [7]. However, learning-based approach enable end-to-end training and optimization, without the need for manual feature engineering or understanding of the underlying data processing mechanisms. Denoising enables the model to learn more robust feature representations that are less sensitive to variations and perturbations and to focus its attention more effectively for more precise object positioning and classification. Meanwhile, the queries sourced from the object list are enriched with raw data feature during cross-attention, and prepared for concatenation with extracted object embedding to the data association module, while DN-DETR discards denoising queries during inference. Introducing multiple denoising groups provides diverse training scenarios with a larger variety of noise levels, which accelerates the convergence and also prevents the overfitting to the GT-like data.

Moreover, DN-DETR highlights that feeding ground truth-like information directly into the Transformer during training can cause over-reliance, degrading performance during inference. Hence, an extra attention mask regulating the visibility of two parts of queries is incorporated into the self-attention mechanism in the decoder to prevent information leakage [20]. In QDN, we discard the attention mask which prevents the self attention so that the detection queries can get useful information from the denoising part. The co-occurrence between raw data and object list facilitate the prediction of objects on raw data.

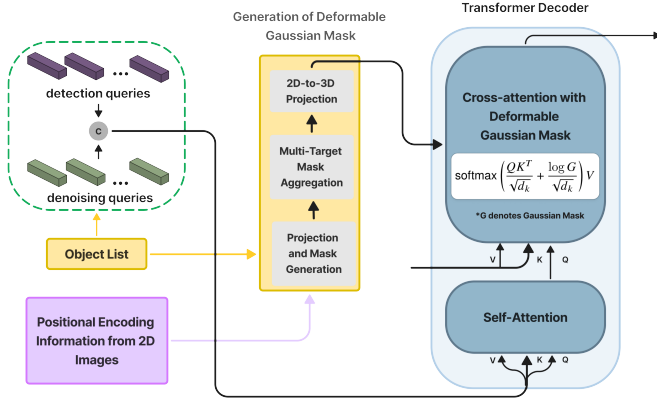


Fig. 3: The structure of the deformable multi-view, multi-target shared Gaussian mask generation and its implementation in the Transformer decoder. Object list information is combined with positional encoding information from 2D images captured by the camera. Our SMCA approach generates Gaussian masks and transits these reshaped Gaussian masks to the cross-attention module, refining the attention mechanism by reweighting the attention maps.

B. Explicit Attention Directing

In addition to implicitly learning through the attention mechanism, we utilize a deformable Gaussian mask to adjust positional attention during cross attention, inspired by Spatially Modulated Co-Attention (SMCA) [21]. SMCA creates a soft link between the object list and the raw image data to dynamically emphasize relative position during the learning process.

While the SMCA approaches referenced in [16], [21] establish a one-to-one alignment between queries and targets constrained by a Gaussian mask around the initial query, PETRv2 generates a large amount of random queries without predefined links to the Gaussian circles around targets. To solve this issue, we implement a one-to-many assignment of detection queries to targets within the Gaussian mask. This allows queries to map to any target or even a no-object class after training.

Fig. 3 provides a detailed flowchart of the process to compute and integrate the Gaussian mask into the Transformer decoder. Initially, object position data from the object lists and position encoding of objects in the 2D images are ported to the mask generator. With the projection matrices of cameras, we project their corresponding positions in multi-view images, subsequently resulting in a 2D Gaussian weighting mask M for each target. The mask generation process resembles the one applied in [22]:

$$M_{ij} = \exp\left(-\frac{(i - cx)^2 + (j - cy)^2}{\sigma * r^2}\right), \quad (1)$$

where (i, j) representing the mask's spatial indices, (cx, cy) as the 2D projected center, r as the bounding box radius, and σ as a parameter controlling Gaussian distribution bandwidth.

The individual masks for each target within an image are combined to form a multi-target shared Gaussian mask. The merge mask is then reshaped and transmitted to the 3D space. The attention reweighting between queries and feature maps involves element-wise addition of Gaussian weights to the cross-attention map across all attention heads. Consequently, the deformable Gaussian masks refine the attention mechanism, allowing each detection query to precisely concentrate on image areas that include projected targets from the object list.

For the modified attention reweighting mechanism, we reformulate the corresponding expression:

$$\text{Attention}(Q, K, V) = \text{softmax}\left(\frac{QK^T}{\sqrt{d_k}} + \frac{\log G}{\sqrt{d_k}}\right)V, \quad (2)$$

where G denotes our Gaussian masks. we incorporate a logarithmic function to prevent extreme values in Gaussian mask from overpowering the overall attention score without introducing negatives to attention map. This helps to control the attention scores of specific positions, ensuring they do not become excessively large and dominate the overall prediction. Additionally, we retain the operation of dividing by $\sqrt{d_k}$ from the original attention score calculation to improve model stability and training efficiency.

IV. EXPERIMENTS

A. Experimental Setup

a) *Dataset*: We chose the nuScenes dataset [9] as our experimental data source, which is a popular benchmark widely used for 3D object detection and multi-object tracking tasks in large-scale autonomous driving. The nuScenes dataset provides synchronized data from 6 cameras surrounding the ego car, capturing 10 object categories for detection and 7 moving classes for tracking in a 360°-field of view at a frequency of 12Hz. It contains 700, 150 and 150 scenes respectively in the training, validation and test sets.

b) *Data Preparation*: Our model and data processing pipeline are based on the MMDetection3D [23] framework, facilitating efficient code development. Besides the multi-view images, the 3D annotations are imported into our training/testing pipeline with MMDetection3D to generate pseudo-object lists. We manually adopted a unified setup for all training experiments regarding the object list generation with max noise standard deviation ratio of 0.06, max drop rate of 0.2, max false positive rate of 0.1, and max label change rate of 0.3.

c) *Implementation Details*: Our framework adopted detection baseline PETRv2 with modified denoising implementation and SMCA. In particular, we utilize 6 Nvidia RTX A5000 GPUs with 24GB of RAM in our experiments. The model is trained with a batch size of 1 due to the memory limit of the GPU for 24 epochs. we employ the AdamW optimizer with an initial learning rate of 2.0×10^{-4} . By default, the number of queries and threshold parameters for detection stay the same as baseline.

Detection	Backbone	NDS \uparrow	mAP \uparrow	mATE \downarrow	mASE \downarrow	mAOE \downarrow	mAVE \downarrow	mAAE \downarrow
PETrv2 [18]	V2-99	0.4038	0.4136	0.7208	0.7094	1.5492	0.4084	0.1914
our model	V2-99	0.5685	0.5499	0.6334	0.2558	0.5006	0.4860	0.1885

TABLE I: Comparison of cross-level fusion with baselines on the nuScenes val set. Image resolution of 800×320 as the inputs.

Model	w Object Lists		w/o Object Lists	
	mAP \uparrow	NDS \uparrow	mAP \uparrow	NDS \uparrow
DN-PETrv2	0.139	0.324	0.419	0.507
QDN-PETrv2	0.491	0.526	0.287	0.404
SMCA-QDN-PETrv2	0.550	0.569	0.299	0.416

TABLE II: Robustness of the cross-level fusion framework against loss of the modality of object lists. DN, QDN and SMCA denotes respectively original Denoising mechanism, Query DeNoising, and Spatially Modulated Co-Attention.

Model	Modules		Detection Metrics	
	QDN	SMCA	NDS \uparrow	mAP \uparrow
PETrv2			0.4104	0.5025
QDN	✓		0.4905	0.5255
SMCA-QDN	✓	✓	0.5499	0.5685

TABLE III: The results of a step-by-step ablation study to evaluate the performance improvements of our proposed model over the baseline. The study involved progressively introducing different components of our framework.

B. Experimental Results

1) *Comparison to Baseline*: Tab. I exhibits the detection performance of our cross-level fusion framework over the vision-based baseline. Our model shows substantial improvements over the baseline models in most key performance metrics with the trade-offs of a decrease in velocity estimation accuracy (mAVE). The degraded velocity estimation may originate from the lack of velocity denoising, when the DN-queries only focus on position and size. A potential solution is to extend query initialization to incorporate velocity perturbation and refinement, which could improve motion estimation while maintaining strong detection accuracy. These results suggest that SMCA and QDN enhancements are generally effective and incorporating high-level information early in the feature level can significantly improve overall performance of the object detection with raw sensor data.

2) *Ablation Study*: Here we explore the effect of two key components in our design: query denoising (QDN) and explicit prior integration in attention mechanism with SMCA. As shown in Tab. III, with QDN, PETrv2 already improves the detection performance by 8.01% NDS and 2.30% mAP. With SMCA, the performance is further improved by 5.94% NDS and 4.30% mAP, which shows a large margin compared to the baseline. The results confirm the synergistic benefits of combining implicit cooperation of object list information via QDN and explicit prior integration with SMCA in our framework. QDN improves detection performance, supporting our assumption that it enhances detection efficiency. While SMCA also brings significant benefits, its impact primarily comes from better feature alignment and attention guidance. Both modules add minimal overhead, as QDN replace part of the original queries without increasing total amount and Gaussian mask generation is efficiently implemented and scales linearly with the typically small object number (< 50).

3) *Robustness against Modality Loss*: From an engineering perspective, when raw data is unavailable, the object list should be directly forwarded to the decision-making module. There-

fore, we define modality loss here as the absence of object lists. QDN differs from DN by removing the attention mask regulating the visibility between DN-queries and randomly-initialized queries. The significant performance drop in detection, a decrease by 25% in mAP on our model under the absence of object lists, shows the reliability of Transformer decoder on the DN-queries during inference. Interestingly, the explicit prior integration via SMCA can slightly mitigate the degeneration. However, this strong sensitivity to presence of object lists is worthy of further exploration. A potential solution is to introduce masked-modality training as in CMT [24], where object lists are randomly masked during training. While we have not yet implemented this, future work could investigate its effectiveness in improving robustness to missing object lists. Additionally, we investigate the direct application of the original denoising mechanisms for the fusion of object lists. However, the results were unexpectedly suboptimal. When incorporating auxiliary high-level modal information into DN-queries during inference, the performance degradation was even more pronounced than with QDN without object lists. When injecting denoised queries during inference, the learnable queries may deviate from their intended targets.

4) *Generalization with Real and Synthetic Object Lists*: The findings in Tab. IV demonstrate our model’s generalization capacity across different object list sources. With synthetic object lists, performance correlates directly with noise levels, while maintaining robustness under moderate noise conditions. To validate our approach with realistic detections, we conducted experiments using object lists from actual 3D detectors. With CenterPoint [25] (mAP 0.564, NDS 0.652), CLF achieves performance (mAP: 0.469, NDS: 0.531) comparable to moderate-noise synthetic data. PointPillars [26], with lower performance (mAP: 0.343, NDS: 0.491), still provides significant improvements on NDS over the vision-only baseline. These results confirm both the effectiveness of our cross-level fusion approach with real detector outputs and the fidelity of our POLG noise parameters as reasonable approximations of

Object List Source	mAP \uparrow	NDS \uparrow
POLG (0.03, 0.1, 0.05, 0.1)	0.590	0.593
POLG (0.06, 0.2, 0.1, 0.3)	0.550	0.569
POLG (0.1, 0.3, 0.2, 0.5)	0.487	0.530
CenterPoint (0.564/0.652)	0.469	0.531
PointPillars (0.343/0.491)	0.387	0.478

TABLE IV: Generalization capability with different object list sources. For PLOG lists, the parameters follow (std, drop, FP, label noise) format. Bold indicates settings used in training. For real detector, the mAP/NDS scores are reported.

actual detector behavior.

V. CONCLUSION

Object lists contain high-level object information typically fused at the decision level. Our cross-level fusion approach introduces this high-level information into the low-level feature extraction process for 3D object detection. The denoising mechanism enhances the model’s ability to learn resilient features, thereby improving positional accuracy. Explicit integration of positional and size information as Gaussian masks directs attention towards specific target regions. Experimental results on the nuScenes dataset demonstrate that incorporating object lists into vision-based methods significantly enhances detection accuracy. This validates the effectiveness of our model in bridging high-level and low-level fusion. Furthermore, our approach is adaptable and can be extended beyond detection. Future work will integrate velocity-aware DNF and temporal attention to improve velocity estimation and robustness to absent object lists through consistent temporal modeling. Additionally, we plan to investigate adaptive fusion strategies, where the model learns to weigh object list information based on reliability, reducing the impact of noisy detections and extend our fusion framework to multi-object tracking. Finally, comparison against traditional high-level fusion methods will be crucial to further assess its practical applicability in autonomous driving.

REFERENCES

- [1] F. Castanedo, “A review of data fusion techniques,” *The Scientific World Journal*, vol. 2013, no. 1, p. 704504, 2013. [Online]. Available: <https://onlinelibrary.wiley.com/doi/abs/10.1155/2013/704504>
- [2] S. C. Thomopoulos, R. Viswanathan, and D. C. Bougoulas, “Optimal decision fusion in multiple sensor systems,” *IEEE Transactions on Aerospace and Electronic Systems*, vol. AES-23, no. 5, pp. 644–653, 1987.
- [3] H. Chen, T. Kirubarajan, and Y. Bar-Shalom, “Performance limits of track-to-track fusion versus centralized estimation: theory and application [sensor fusion],” *IEEE Transactions on Aerospace and Electronic Systems*, vol. 39, no. 2, pp. 386–400, 2003.
- [4] C.-Y. Chong, “Tracking and data fusion: A handbook of algorithms (barshalom, y. et al; 2011) [bookshelf],” *IEEE Control Systems Magazine*, vol. 32, no. 5, pp. 114–116, 2012.
- [5] M. Ambrosin, L. L. Yang, X. Liu, M. R. Sastry, and I. J. Alvarez, “Design of a misbehavior detection system for objects based shared perception v2x applications,” in *2019 IEEE Intelligent Transportation Systems Conference (ITSC)*. IEEE, 2019, pp. 1165–1172.
- [6] B. Spencer Jr, M. E. Ruiz-Sandoval, and N. Kurata, “Smart sensing technology: opportunities and challenges,” *Structural Control and Health Monitoring*, vol. 11, no. 4, pp. 349–368, 2004.

- [7] S. Matzka and R. Altendorfer, “A comparison of track-to-track fusion algorithms for automotive sensor fusion,” in *2008 IEEE International Conference on Multisensor Fusion and Integration for Intelligent Systems*, 2008, pp. 189–194.
- [8] C.-Y. Chong, S. Mori, W. Barker, and K.-C. Chang, “Architectures and algorithms for track association and fusion,” *IEEE Aerospace and Electronic Systems Magazine*, vol. 15, no. 1, pp. 5–13, 2000.
- [9] H. Caesar, V. Bankiti, A. H. Lang, S. Vora, V. E. Liong, Q. Xu, A. Krishnan, Y. Pan, G. Baldan, and O. Beijbom, “nuscenes: A multimodal dataset for autonomous driving,” in *Proceedings of the IEEE/CVF conference on computer vision and pattern recognition*, 2020, pp. 11 621–11 631.
- [10] C. Y. Chong, S. Mori, W. H. Barker, and K. C. Chang, “Architectures and algorithms for track association and fusion,” *IEEE Aerospace and Electronic Systems Magazine*, vol. 15, no. 1, pp. 5–13, 2000.
- [11] K. Huang, B. Shi, X. Li, X. Li, S. Huang, and Y. Li, “Multi-modal sensor fusion for auto driving perception: A survey,” *arXiv preprint arXiv:2202.02703*, 2022.
- [12] R. Girshick, J. Donahue, T. Darrell, and J. Malik, “Rich feature hierarchies for accurate object detection and semantic segmentation,” in *Proceedings of the IEEE conference on computer vision and pattern recognition*, 2014, pp. 580–587.
- [13] X. Chen, H. Ma, J. Wan, B. Li, and T. Xia, “Multi-view 3d object detection network for autonomous driving,” in *Proceedings of the IEEE conference on Computer Vision and Pattern Recognition*, 2017, pp. 1907–1915.
- [14] J. Ku, M. Mozifian, J. Lee, A. Harakeh, and S. L. Waslander, “Joint 3d proposal generation and object detection from view aggregation,” in *2018 IEEE/RSJ International Conference on Intelligent Robots and Systems (IROS)*. IEEE, 2018, pp. 1–8.
- [15] X. Chen, T. Zhang, Y. Wang, Y. Wang, and H. Zhao, “Futr3d: A unified sensor fusion framework for 3d detection,” in *proceedings of the IEEE/CVF conference on computer vision and pattern recognition*, 2023, pp. 172–181.
- [16] X. Bai, Z. Hu, X. Zhu, Q. Huang, Y. Chen, H. Fu, and C.-L. Tai, “Transfusion: Robust lidar-camera fusion for 3d object detection with transformers,” in *Proceedings of the IEEE/CVF conference on computer vision and pattern recognition*, 2022, pp. 1090–1099.
- [17] X. Xu, S. Dong, T. Xu, L. Ding, J. Wang, P. Jiang, L. Song, and J. Li, “Fusionrcnn: Lidar-camera fusion for two-stage 3d object detection,” *Remote Sensing*, vol. 15, no. 7, p. 1839, 2023.
- [18] Y. Liu, J. Yan, F. Jia, S. Li, A. Gao, T. Wang, and X. Zhang, “PetrV2: A unified framework for 3d perception from multi-camera images,” in *Proceedings of the IEEE/CVF International Conference on Computer Vision*, 2023, pp. 3262–3272.
- [19] Y. Lee and J. Park, “Centermask: Real-time anchor-free instance segmentation,” in *Proceedings of the IEEE/CVF Conference on Computer Vision and Pattern Recognition (CVPR)*, June 2020.
- [20] F. Li, H. Zhang, S. Liu, J. Guo, L. M. Ni, and L. Zhang, “Dn-detr: Accelerate detr training by introducing query denoising,” in *Proceedings of the IEEE/CVF Conference on Computer Vision and Pattern Recognition*, 2022, pp. 13 619–13 627.
- [21] P. Gao, M. Zheng, X. Wang, J. Dai, and H. Li, “Fast convergence of detr with spatially modulated co-attention,” in *Proceedings of the IEEE/CVF international conference on computer vision*, 2021, pp. 3621–3630.
- [22] X. Zhou, D. Wang, and P. Krähenbühl, “Objects as points,” in *arXiv preprint arXiv:1904.07850*, 2019.
- [23] M. Contributors, “MMDetection3D: OpenMMLab next-generation platform for general 3D object detection,” <https://github.com/open-mmlab/mmdetection3d>, 2020.
- [24] J. Yan, Y. Liu, J. Sun, F. Jia, S. Li, T. Wang, and X. Zhang, “Cross modal transformer: Towards fast and robust 3d object detection,” in *Proceedings of the IEEE/CVF international conference on computer vision*, 2023, pp. 18 268–18 278.
- [25] T. Yin, X. Zhou, and P. Krahenbuhl, “Center-based 3d object detection and tracking,” in *Proceedings of the IEEE/CVF conference on computer vision and pattern recognition*, 2021, pp. 11 784–11 793.
- [26] A. H. Lang, S. Vora, H. Caesar, L. Zhou, J. Yang, and O. Beijbom, “Pointpillars: Fast encoders for object detection from point clouds,” in *Proceedings of the IEEE/CVF conference on computer vision and pattern recognition*, 2019, pp. 12 697–12 705.